Stress and dislocations in thin metal layers

Nicola, Lucia

Chapter 3

Two hardening mechanisms in single crystal thin films *

Even though it is widely accepted that thin film hardening is thickness dependent (see, e.g., [1]), a universal scaling law to describe the phenomenon has not yet been found. Many authors propose to use a Hall-Petch relation, of the type used for bulk materials, where the grain size d is replaced by the film thickness h. The exponent of h, however, is still unknown. What has been often proposed is that the film strength scales inversely with the film thickness ([2, 3, 4]), but experiments are not decisive. Beside the practical difficulty of performing experiments on very thin films, available experimental results have the drawback that it is hard to distinguish between the contribution of grain size and of film thickness on hardening.

As shown in the previous chapter, discrete dislocation simulations on single crystal thin films are able to capture a size-dependent response in films thinner than roughly one micrometer. There, we have mainly attributed the size effect to the presence of a hard boundary layer of non-scaling thickness at the film-substrate interface, caused by dislocation pile-ups. However, a Hall-Petch like scaling law with a coefficient common to the three films considered was not found, suggesting that a constant boundary layer is not the only cause of the size effect. The high stress found in the thinnest film analyzed in chapter 2, $h = 0.25\mu$m, was explained by a different origin of hardening in such thin films.

In this chapter, attention is focused on films with thickness ranging from 2 to 0.125 μm. In particular we study the difference in hardening of thin versus very thin films as found in dislocation dynamics simulations, through a straightforward analysis of how the dislocation structure is related to the film stress state. Simulations show that there is a material-dependent threshold thickness below which the size effect is completely determined by the capability of Frank-Read sources

*Based on *Two hardening mechanisms in single crystal thin films studied by discrete dislocation plasticity*, L. Nicola, E. Van der Giessen, A. Needleman, Philos. Mag., to appear.

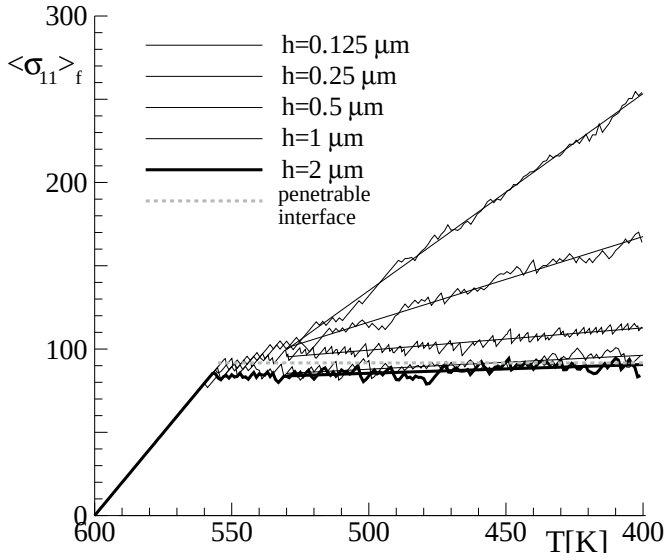

Figure 3.1 Average stress in the film, $\langle\sigma_{11}\rangle_{\rm f}$, versus temperature T for films of various thickness.

to operate in a constrained geometry. Only above this threshold thickness, is the size effect due to the non-scaling size of the boundary layer.

3.1 Observations from simulations

Results are presented for five films of thickness $h = 2$, 1, 0.5, 0.25 and 0.125μm. Formulation of the problem and method of analysis are the same used in the previous chapter. The simulation parameters are also unchanged, with exception of the average nucleation strength $\tau_{\rm nuc}$ and standard deviation $\tau_{\rm ave}$, which are here taken to be 50 and 10MPa, respectively (they were 25 and 5MPa in chap. 2). A larger nucleation strength gives a shorter nucleation length $L_{\rm nuc}$, which is more appropriate in the study of a film as thin as 0.125μm, since $L_{\rm nuc}$ should be completely contained in the film.

The major part of the discussion will be for a crystal with slip plane orientation $\phi^{(60)} = (0^\circ, 60^\circ, 120^\circ)$ but we will also consider slip planes with orientation $\phi^{(30)} = (30^\circ, 90^\circ, 150^\circ)$.

The curves in Fig. 3.1 show the evolution of the average in-plane stress, $\langle\sigma_{11}\rangle_f$, during cooling in the different films, for which the interface with the substrate is

impenetrable for the dislocations. Plastic relaxation by dislocation motion is quite effective in all films until a temperature of around 530K is reached: there is a size effect, but it is not as pronounced as during the rest of the cooling. For $T < 530$K the thinnest two films harden linearly with a larger slope and the size effect becomes more evident. The change in slope corresponds to the formation of dislocation pile-ups at the film-substrate interface, which influence relaxation through their back stress on the sources, as discussed in some detail in chapter 2. Between $T \approx 530$K and the final temperature, $T = 400$K, the curves have been fitted to straight lines according to a standard least-squares algorithm.

The gray line in Fig. 3.1 fits the average stress-temperature curve for a film with $h = 0.5\mu$m which has a completely absorbing interface with the substrate. In this case, dislocations can pass through the interface where they are absorbed into the substrate, leaving displacement steps accommodated by the substrate. Also in this case, yield occurs when the weakest source in the film nucleates, but after yield, plastic flow continues at the yield stress. After nucleation, dislocation pairs glide the slip planes until one dislocation leaves the film from the free surface and the other enters the absorbing interface. Dislocations do not accumulate in the film as in the case of films with impenetrable interface, and therefore there is no back stress, no hardening and no size effect.

Figure 3.2 shows how the stress σ_{11} averaged along the x_1 direction varies over the film height. $\langle\sigma_{11}\rangle$ is uniform in the film with a perfectly absorbing interface with the substrate. All other films exhibit a hard layer in proximity of the film-substrate interface and an almost homogeneous stress state in the rest of the film. The hard layer is characterized by a high stress gradient towards the interface.

The line indicating the stress profile in the film with an absorbing interface intersects the curves for the three thicker films. We take this intersection as the separation point between the hard boundary layer and the zone of homogeneous stress in these films. In the following we will refer to the zone of homogeneous stress between boundary layer and free surface as bulk. For the two thinner films, we define the bulk as the zone at constant stress close to the free surface, the boundary layer the zone close to the interface were there is a stress gradient. While the three thicker films have approximately the same value of stress in the bulk ($\langle\sigma_{11}\rangle_b \simeq 80$MPa), the bulk of the two thinner films is much harder ($\langle\sigma_{11}\rangle_b = 145$MPa for the film with $h = 0.25\mu$m and $\langle\sigma_{11}\rangle_b = 245$MPa for the film with $h = 0.125\mu$m). The size of the boundary layer is approximately the same in the two thicker films ($h_l = 0.25\mu$m), but is smaller in the two thinner ones (approximately

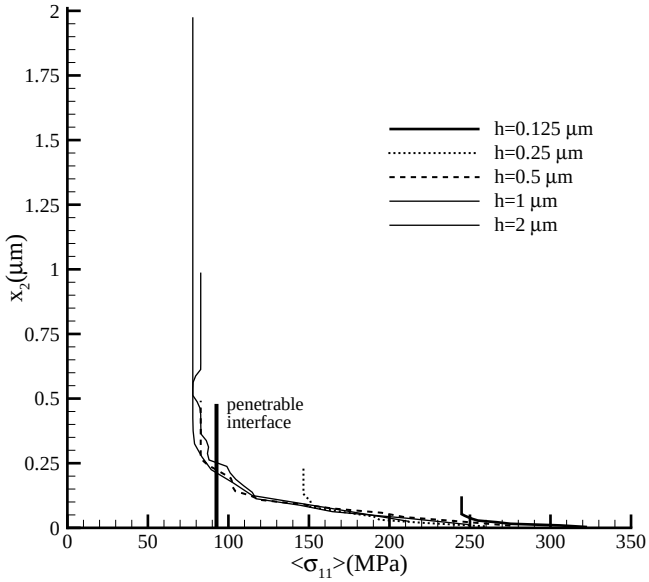

Figure 3.2 Distribution of the average in-plane stress $\langle\sigma_{11}\rangle$ over the film height x_2 in films with an impenetrable interface. The result for a $h = 0.5\mu$m film with an absorbing interface is shown for comparison.

$h_l = 0.1\mu$m for $h = 0.25\mu$m and $h_l = 0.05\mu$m when $h = 0.125\mu$m). The thinnest film considered is actually thinner than the boundary layer in the thicker films.

Figure 3.3 shows the stress state reached at final temperature and the corresponding dislocation distribution for the films with $h = 0.5$ and $h = 0.125\mu$m. Black dots indicate the positions of Frank-Read sources (recall that their density is independent of h). The stress is normalized by the elastic stress

$$\sigma_{\rm n} = E/(1-\nu^2)\varepsilon_{th} = -\Delta\alpha E\Delta T/(1-\nu)$$

which for $\Delta T = -200K$ is $\sigma_{\rm n} = 397$MPa. For a given range of contour levels, a comparison can be made between the stress state in the two films. Two differently stressed regions can be recognized in the thicker film. But, a measure of the size and intensity of the boundary layer cannot be obtained from these contour plots since the size of the white region in the thicker film depends on the contour levels and range.

The analysis of the dislocation structure at final temperature can give a better understanding of the stress profiles in Fig. 3.2. What is common to the two films

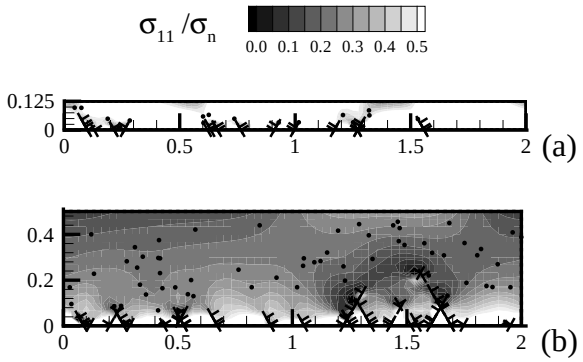

Figure 3.3 Distribution of dislocations ($\perp$) and sources ($\bullet$) in films of thickness (a) $h = 0.125\mu$m and (b) $h = 0.5\mu$m at final temperature, superimposed on contours of constant σ_{11}.

in fig 3.3 is that dislocations have piled up against the film-substrate interface and that only the slip planes at 60° and 120° have been active. The main differences between the dislocation structures of the two films are the dislocation density, the density of dislocation pile-ups and their length. These quantities are listed for the five films considered in Table 3.1, together with the average stress in the films and the stress computed in the film bulk. One notes first that the density of dislocations for the film with $h = 1\mu$m is two times larger than in the film with $h = 2\mu$m; the same holds for the films with $h = 0.5$ and 1μm but for the two thinner films the dislocation density does not scale any more with the film thickness. This means that in the thinner films a smaller number of dislocation pairs has been available to relax the stress during thermal history, explaining the higher average stress in these films (see also [5]). A reduced nucleation activity in very thin films is caused by the proximity of sources to the film-substrate interface: the length of dislocation pile-ups is then limited by the distance between the point source and the interface. The longest pile-up in the film of thickness $h = 1\mu$m is 0.25μm long. Such a long pile-up can surely not form in a film with $h = 0.125\mu$m. In addition to that, sources that are very close to the interface and thus to the dislocation pile-ups, are affected by the back stress associated to the pile-ups, which delays the nucleation events [5]. The back stress affecting a source close to the interface is mainly caused by the pile-up generated by the nucleation source itself. In the subsequent sections we will analyze more in detail how the dislocation structure at final temperature is related to the stress state in the film.

$h(\mu\text{m})$	0.125	0.25	0.5	1	2
average stress $\langle\sigma_{11}\rangle$ (MPa)	253	167	113	96	90
bulk stress $\langle\sigma_{11}\rangle_b$ (MPa)	245	147	82	82	78
dislocation density (μm^{-2})	124	102	64	33	16.5
pile-up density (μm^{-2})	56	40	18	8	4.5
max pile-up length (μm)	0.045	0.115	0.221	0.250	0.312
boundary layer thickness (μm)	0.05	0.13	0.250	0.245	0.245
σ_b (MPa) from (3.4)	246	150	86	87	77
σ_{int} (MPa) from(3.6)	330	300	310	319	310

Table 3.1 Characteristics in films with slip planes at $(0^\circ, 60^\circ, 120^\circ)$ at various values of the film thickness.

3.2 Characterization of stress state

3.2.1 Stress state in the film bulk

As shown in Fig. 3.2, the stress at final temperature in the bulk of all films is homogeneous and lower than the elastic stress, $\sigma_n = 397$MPa. The stress in the bulk has been relaxed by dislocation pairs that have glided during thermal history. One dislocation out of each pair has left the film through the free surface but the other is still in the film, piled up against the interface. The density of dislocations that have contributed to the relaxation of the film is therefore known from the final dislocation density.

Stress relaxation is mainly given by dislocation glide on the slip planes with $\phi = 60^\circ$ and $\phi = 120^\circ$. Dislocation activity on the slip planes parallel to the interface is very limited, since their Schmid factor is zero. Figure 3.4(a) gives a schematic representation of the relaxation process: opposite signed dislocations move on the slip planes, one towards the free surface, the other towards the interface with the substrate. The dislocations in Fig. 3.4(a) can be approximated by two parallel arrays of dislocations, each having Burgers vector of length $b\cos\phi$ but pointing in x_1 or $-x_1$ direction, respectively.

The stress field of a single array of dislocations in infinite space (see Fig. 3.5)

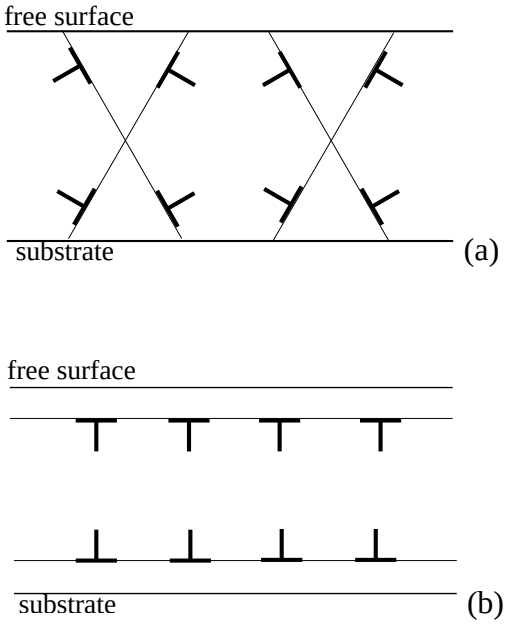

Figure 3.4 (a) Schematic representation of dislocations gliding on slip planes $\phi = 60^\circ$ and $\phi = 120^\circ$. (b) Dislocation structure equivalent to the one in figure (a), obtained by composing the dislocation Burgers vectors. The Burgers vector of each dislocation in the array is $b\cos\phi$.

can be calculated analytically (see for the complete derivation [6]):

$$\sigma_{11} = \frac{Eb}{4d(1-\nu^2)} \frac{1}{\cosh 2\pi\eta - \cos 2\pi\xi} \left[2\sinh 2\pi\eta + 2\pi\eta \frac{1-\cos 2\pi\xi \cosh 2\pi\eta}{\cosh 2\pi\eta - \cos 2\pi\xi} \right], \tag{3.1}$$

where d is the spacing between dislocations, and $\xi = X/d$ and $\eta = Y/d$ are local coordinates of the point were σ_{11} is calculated (see Fig. 3.5). This stress, averaged over ξ for any value of $\eta > 0$, is

$$\langle \sigma_{11} \rangle_\xi (\eta) = -\frac{Eb\cos\phi}{2d(1-\nu^2)}. \tag{3.2}$$

The effect of the array near the free surface is the same, so that the average stress between the two arrays of dislocations in Fig. 3.4b is given by

$$\sigma_d = -\frac{Eb\cos\phi}{d(1-\nu^2)}. \tag{3.3}$$

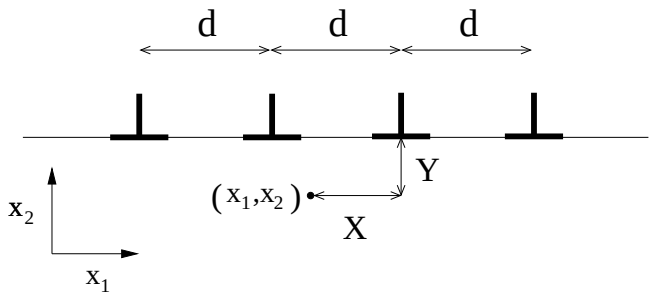

Figure 3.5 Infinite array of edge dislocations spaced by d.

On average, the effects of the two arrays outside the band cancel. If the dislocation arrays are moving in a film, the stress state in the part of the film already glided is $\sigma_n + \sigma_d$, in the rest of the film it is just the elastic stress. The relaxation process is complete when one of the arrays reaches the interface and the other one the free surface. The average stress state then is $\sigma_n + \sigma_d$ everywhere in the film, i.e.

$$\sigma_b = \sigma_n - \frac{Eb\cos\phi}{d(1-\nu^2)} = \sigma_n - \frac{\rho h E b\cos\phi}{(1-\nu^2)} \tag{3.4}$$

where ρ is the density of dislocations in the film.

The same result can be obtained by considering each dislocation at the interface as an inserted atomic half plane of Burgers vector $b\cos\phi$. The plastic strain caused by an array of such half planes at a spacing d is $\varepsilon_p = b\cos\phi/d$. This strain partly accommodates the applied thermal strain ε_{th}. From this argument the bulk stress can be expressed as

$$\sigma_b = \frac{E}{(1-\nu^2)}\left[\varepsilon_{th} - \varepsilon_p\right] = \frac{E}{(1-\nu^2)}\left[(1+\nu)\Delta\alpha\Delta T - \frac{b\cos\phi}{d}\right] \tag{3.5}$$

which is identical to eq. (3.4).

Comparison between the values of σ_b obtained from eq. (3.4) and $\langle\sigma_{11}\rangle_b$ computed during the simulation shows very good agreement. We conclude that the density of dislocations in the quantity ρh together with the orientation of the Burgers vectors is sufficient to determine the average stress state in the film bulk. It is to be noticed that the value of ρh is $32\mu\text{m}^{-1}$ for the thicker films and only $26\mu\text{m}^{-1}$ and $16\mu\text{m}^{-1}$ for the two thinnest ones in Table 3.1. As mentioned before, dislocations nucleated in the thinner films are not sufficient to relax the film bulk as much as in the thicker films.

3.2.2 Stress state in the boundary layer

As previously mentioned we call boundary layer the part of the film close to the interface, were the stress is larger than the stress in the bulk. By comparing Fig. 3.2 and Fig. 3.3 one can see that the size of this boundary layer is determined by the length of dislocation pile-ups, see also Table 3.1. The $\langle\sigma_{11}\rangle(x_2)$ stress is maximum at the interface, where the first dislocations of the pile-ups are located. At the interface, only the effect of those dislocations is present. The dislocation array formed by the first dislocations of all pile-ups produces a stress state which can again be described by equation (3.3). The stress at the interface can be calculated as:

$$\sigma_{int} = \sigma_n - \frac{\rho_p h E b \cos\phi}{(1-\nu^2)} \tag{3.6}$$

where ρ_p is the density of leading pile-up dislocations at the interface, independently of pile-up length (when present, also single dislocations at the interface).

The values calculated using equation (3.6) (listed in Table 3.1) are somewhat larger than the values one can read from the plot in Fig. 3.2. This is due to the fact that measure in the plot is not very accurate, the stress is not calculated exactly at the interface, but through integration points close to the interface. In this way part of the effect of the second dislocations in the pile-ups is also taken into account. The stress rapidly decreases with the distance from the interface until it reaches the bulk stress. The stress gradient is not constant in the boundary layer, but becomes smaller in proximity to the bulk, were only the last dislocations of a few long pile ups contribute to it. The pile-ups are shorter in the thinner films than in the thicker ones, therefore the boundary layer in very thin films is thinner.

3.2.3 Validity of the Hall–Petch relation

Let us first consider the thicker films, $h \geq 0.5\mu$m. If we assume a hardening law of the type

$$\sigma = \sigma_0 + kh^{-n}, \tag{3.7}$$

we can take $\sigma_0 = \sigma_b \cong 80$ MPa, since the thicker films have a similar stress state in the bulk. We first obtain the coefficient k by substituting in (3.7) the values of $\langle\sigma\rangle$ and $\langle\sigma\rangle_b$ for the film with $h = 1\mu$m at final temperature. For this film thickness, knowledge of n is not needed and we find $k = 16\text{MPa}\mu\text{m}^n$. With this value of k, substitution of the values of $\langle\sigma_{11}\rangle$ for σ and $\langle\sigma_{11}\rangle_b$ for σ_b for the film with $h = 0.5\mu$m, yields that the exponent of h must be $n = 1$. As a check we can use

the film of thickness $h = 2\mu$m: substitution of the obtained values into (3.7) leads to $\sigma = 88$MPa which is very close to the value of $\langle\sigma_{11}\rangle = 90$MPa obtained from the simulation, see Table 3.1.

The average stress in the film can be more specifically seen as the weighted sum of the stress in the film bulk and the average stress in the boundary layer, i.e.

$$\sigma = \sigma_b \frac{1-h_l}{h} + \sigma_l \frac{h_l}{h}, \tag{3.8}$$

where σ_l and h_l indicate the boundary layer average stress and thickness, respectively. Equation (3.8) can be rewritten to have the form of equation (3.7) as

$$\sigma = \sigma_b + (\sigma_l - \sigma_b)h_l/h, \tag{3.9}$$

so that $k = (\sigma_l - \sigma_b)h_l$ and $n = 1$.

The equation (3.9) holds for films of any thickness. For the three thicker films, k and $\langle\sigma\rangle_b$ can be considered material parameters, since these films have a similar bulk stress and a similar boundary layer stress and thickness. For the thinner films, however, k and $\langle\sigma\rangle_b$ depend on the film thickness: stress in the bulk and in the boundary layer increase with increasing film thickness, while the size of the boundary layer decreases. In effect it means that the Hall-Petch is no longer relevant.

It is not possible to find a precise film thickness, above which the films will behave according to equation (3.7) with a constant k and σ_b. All parameters which affect the dislocation density in the films, such as the density or strength of nucleation sources or the presence of obstacles, determine at which film thickness k and σ_b will start being dependent on h.

3.3 Crystal orientation

The response of the single crystal depends on its orientation. Figure 3.6 shows the stress profiles for the simulations of four films of thickness ranging from 0.125 to 1μm and slip plane orientation $\phi^{(30)} = (30^\circ, 90^\circ, 150^\circ)$. Table 3.2 summarizes characteristics of the results, similar to Table 3.1.

Comparison of Tables 3.1 and 3.2 shows that the average and bulk stress in the single crystals with $\phi^{(30)}$ is for all film thicknesses lower than in the crystals with $\phi^{(60)}$. Nevertheless, the dislocation densities for the $\phi^{(30)}$ films are lower than in the films with $\phi^{(60)}$. This means that for $\phi = 30^\circ$ a lower dislocation density is

$h(\mu\text{m})$	0.125	0.25	0.5	1
average stress $\langle\sigma_{11}\rangle$ (MPa)	248	114	85	91
bulk stress $\langle\sigma_{11}\rangle_b$ (MPa)	227	91	74	82
dislocation density (μm^{-2})	80	72	40	19
pile-up density (μm^{-2})	24	22	12	4.5
max pile-up length (μm)	0.046	0.094	0.159	0.169

Table 3.2 Characteristics in films with slip planes at $\phi^{(30)}$ at various values of the film thickness.

3.4 Conclusions

Stress relaxation of single-crystal thin films of various thicknesses on a semi-infinite substrate has been simulated using discrete dislocation plasticity. Simulations show that:

- if the film-substrate interface is taken to be perfectly absoring for the dislocations, the stress that the substrate imposes on the film relaxes to a level that depends only on the strength of the weakest nucleation source, independently of the film thickness;
- if the film-substrate interface is impenetrable, stress relaxation is not as efficient as in films with absorbing interface, because dislocations cannot glide into the interface, but pile-up against it, forming a boundary layer characterized by a high stress gradient. The boundary layer is a transition zone between the high stress state at the film-substrate interface and the more relaxed stress state typical of the free surface.
- There is a thickness above which films have a boundary layer with thickness-independent size and average stress. The stress in the rest of the film is very low. Dislocation activity is as intense as in films with a perfectly penetrable interface with the substrate, so that relaxation of the stress in the film bulk is quite good and independent of the film thickness. The size effect in these films is caused by the fact that the size of the boundary layer does not scale with the film thickness.
- In films thinner than a threshold thickness, which depends on the material and on crystal orientation, nucleation is hindered by geometrical con-

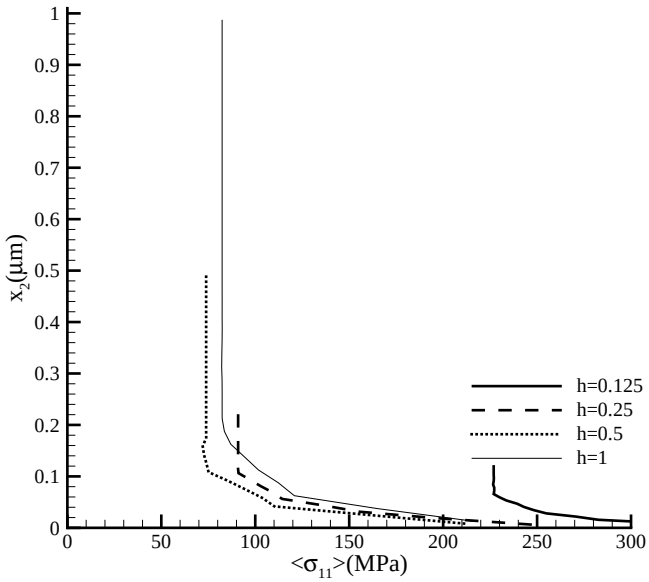

Figure 3.6 Distribution of the average in-plane stress $\langle\sigma_{11}\rangle$ over the film height in films of various thickness with crystal orientation $\phi^{(30)}$.

needed to give the same relaxation. This can be rationalized with equation (3.4): $\cos\phi$ is larger for $\phi = 30^\circ$ than for $\phi = 60^\circ$. Due to the different inclination of the slip planes, the same length of dislocation pile-ups gives a thinner boundary layer for $\phi^{(30)}$ than for $\phi^{(60)}$.

Particularly interesting is the behavior of the film of thickness 0.25μm. In the previous section we have seen that the film stress for $\phi^{(60)}$ does not follow the Hall-Petch relation (3.7) because of insufficient dislocation nucleation. In the $\phi^{(30)}$ orientation, however, fewer dislocations are required for relaxation of the film, so that for this orientation the film does not deviate from the behavior described by (3.7). It should be noticed that for this orientation the stress state in the bulk of the thicker films is approximately the same as in the previous orientation ($\langle\sigma\rangle_b \simeq$ 80MPa), even though there is some more scatter in the results. The coefficient k can be seen as a Taylor coefficient, and has therefore a different value in this orientation. Taking $k = 10$ and $n = 0.5$ in equation (3.8) we find $\sigma = 90$, 94 and 100 MPa for the films with $h = 1$, 0.5 and 0.25μm, respectively, with $\sigma_0 = 80$MPa. If we use for each film $\sigma_0 = \sigma_b$ then $\sigma = 92$, 88 and 111 MPa.

straints, i.e. the vicinity of sources to the interface. The thinner the film, the lower is the dislocation activity. Both the average stress in the boundary layer and the stress in the rest of the film increase with decreasing dislocation density. The size of the boundary layer depends on the length of the pile-ups and scales with the film thickness. So, with decreasing film thickness the boundary layer becomes thinner but the stresses in boundary layer and bulk of the film increase. The size effect in these very thin films is nucleation-controlled and is more pronounced than in the thicker films.

References

[1] E. Arzt **46** (1998) 5611.

[2] W.D. Nix, Scripta Mater. **39** (1998) 545.

[3] R. Venkatraman and J.C. Bravman, J. Mater. Res. **7** (1992) 2040.

[4] L.B. Freund, J. Appl. Mech. **43** (1987) 553.

[5] L. Nicola, E. Van der Giessen, A. Needleman, J. Appl. Phys. **93** (2003) 5920.

[6] E. Van der Giessen, A. Needleman, Simul. Mater. Sci. Eng. **3** (1995) 689.